🅟 Selected for a Viewpoint in *Physics*

PHYSICAL REVIEW LETTERS

Thermodynamics of an Attractive 2D Fermi Gas

K. Fenech, P. Dyke, T. Peppler, M. G. Lingham, S. Hoinka, H. Hu, and C. J. Vale[*]
Centre for Quantum and Optical Sciences, Swinburne University of Technology, Melbourne 3122, Australia

Thermodynamic properties of matter are conveniently expressed as functional relations between variables known as equations of state. Here we experimentally determine the compressibility, density, and pressure equations of state for an attractive 2D Fermi gas in the normal phase as a function of temperature and interaction strength. In 2D, interacting gases exhibit qualitatively different features to those found in 3D. This is evident in the normalized density equation of state, which peaks at intermediate densities corresponding to the crossover from classical to quantum behavior.

Two-dimensional (2D) quantum matter can display behaviors not encountered in three dimensions (3D) [1,2]. Fermions confined to 2D planes play a key role in unconventional superconductors [3], graphene [4], and certain topological insulators [5] yet understanding the properties of these complex materials can present significant theoretical challenges. Simpler systems, such as ultracold atomic gases with tunable interactions [6–8], can serve as valuable test beds for building up and validating models of interacting fermions in 2D. Experiments on 2D Fermi gases to date have addressed their production [9–11], pairing [12,13], pseudogap [14] and polaron physics [15,16], pair condensation [17], the Berezinskii-Kosterlitz-Thouless transition [18], and the pressure [19] as a function of interaction strength at low temperatures. Theoretically, several groups have investigated superfluidity [20–24] and the thermodynamic properties of 2D Fermi gases [25–27]; however, a full experimental characterization remains to be established.

In cold atom experiments, a 2D gas can be produced by subjecting a cloud to tight transverse confinement. In a harmonic potential, with characteristic frequencies ω_x, ω_y, and ω_z, a gas can become kinematically 2D when the transverse (z) confinement energy exceeds all other energy scales including the thermal energy, chemical potential, and interaction energies. The first two criteria require that $\hbar\omega_z \gg k_B T$, E_F where $\hbar$ is Planck's constant, k_B is Boltzmann's constant, T is the temperature, and E_F is the Fermi energy. The criterion for the interactions requires that neither elastic or inelastic (e.g., pair-forming) collisions result in the population of transverse excited states [8,28–32]. At nonzero densities it was found that moderate interactions can lead to transverse excitations, even when $k_B T$ and E_F lie below the transverse oscillator energy [33]. This in turn can impact other parameters such as the pairing gap [34] and superfluid transition temperature [24].

Here we measure the thermodynamic properties of attractive Fermi gases in the normal phase in a parameter regime where 2D kinematics has been clearly established

[33]. We apply a protocol based on the approach used for a 3D Fermi gas at unitarity [35] and employed on a 2D Bose gas [36]. By establishing a model independent relationship between the compressibility and pressure, we extract a range of thermodynamic properties including the temperature, chemical potential, and density equations of state.

In a two-component Fermi gas thermodynamic variables can be expressed as functions, f, connecting the underlying energies within the system [37]. At fixed temperature and interactions, these can be related to the density via the Gibbs-Duhem equation. In 2D the pressure P, density n, and isothermal compressibility κ are given by

$$P = \frac{1}{\beta\lambda^2} f_P(\beta\mu, \beta E_b) = \int_{-\infty}^{\mu} n(\mu', T) d\mu'|_{T, a_{2D}}, \quad (1)$$

$$n\lambda^2 = f_n(\beta\mu, \beta E_b), \quad (2)$$

$$\kappa = \frac{\beta}{(n\lambda)^2} f_\kappa(\beta\mu, \beta E_b) = \frac{1}{n^2} \frac{dn(\mu, T)}{d\mu}\bigg|_{T, a_{2D}}, \quad (3)$$

where $f_i(\beta\mu, \beta E_b)$ depend on the chemical potential μ, temperature and interaction strength, $\beta = 1/(k_B T)$, $\lambda = \sqrt{2\pi\hbar^2/(mk_B T)}$ is the thermal de Broglie wavelength, m is the atomic mass and E_b is the two-body binding energy which in quasi-2D is governed by ω_z and the 3D scattering length a. The 2D scattering length a_{2D} is related to the binding energy by $E_b = \hbar^2/(ma_{2D}^2)$ in the kinematically 2D regime [6,8,28]. Knowledge of the functions f_i represents a complete determination of the thermodynamics and can establish valuable benchmarks for comparison with many-body theories [38].

In the experiments that follow we study 2D atom clouds at thermal equilibrium in a cylindrically symmetric harmonic trap $V_r(x, y) = m\omega_r^2(x^2 + y^2)/2$ with $\omega_r(= \omega_x = \omega_y) \ll \omega_z$. Because of the slowly varying radial potential we can make use of the local density approximation (LDA) which asserts that local thermodynamic properties will be equivalent to those of a
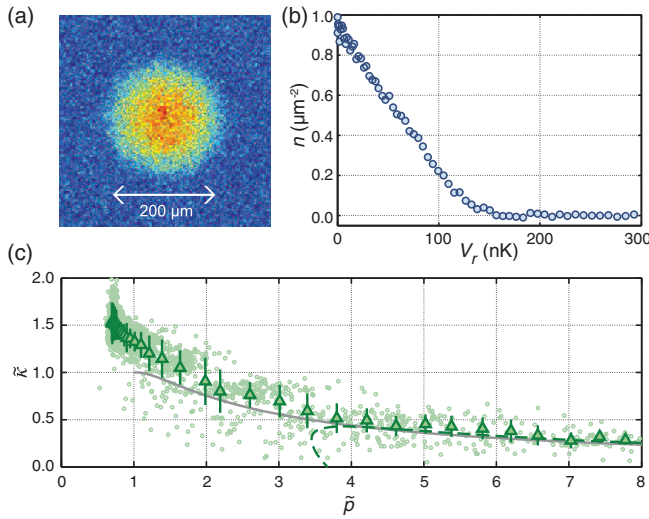
(a)

(b)

(c)

FIG. 1.   (a) Average of 10 absorption images of a 2D Fermi gas, with $\beta E_b = 0.26$, prepared under the same experimental conditions ($B = 880$ G, $N = 16,000$, $T \approx 25$ nk) (b) Azimuthally averaged density, $n(V_r)$, obtained from image (a) as a function of the local potential. (c) Dimensionless compressibility $\tilde{\kappa}$ vs dimensionless pressure $\tilde{p}$ of a 2D Fermi gas with $\beta E_b = 0.26(2)$. Faint green circles show data extracted from single images and dark green triangles are data binned according to $\tilde{p}$. Grey solid line shows the equation of state for a noninteracting Fermi gas and dashed green line is the predicted $\tilde{\kappa}$ based on the virial expansion to third order.

homogeneous gas at the same temperature and chemical potential [39]. Under the LDA the atomic density can be written as $n[\mu(x, y), T]$, where $\mu(x, y) = \mu_0 - V_r(x, y)$ and μ_0 is the chemical potential at the trap center. In any single realization of the experiment, the parameters β and E_b will be fixed across the cloud such that Eqs. (1)–(3) yield $f_n(\beta\mu, \beta E_b) = f'_P(\beta\mu, \beta E_b)$ and $f_\kappa(\beta\mu, \beta E_b) = f''_P(\beta\mu, \beta E_b)$ by differentiation with respect to $\beta\mu$.

We prepare single 2D clouds of neutral ^{6}Li atoms in a hybrid optical-magnetic trap at temperatures in the range of 20–60 nK [33,40–42]. A blue-detuned TEM_{01} mode laser beam provides tight confinement along z with $\omega_z/(2\pi) = 5.15$ kHz. Radial confinement arises from residual magnetic field curvature present when the Feshbach magnetic field is applied, leading to a highly harmonic and radially symmetric potential with $\omega_r/(2\pi) = 26$ Hz with an anisotropy of less than 0.6%. We image along z to directly obtain the density $n(x, y)$ of clouds prepared in the kinematically 2D regime. Figure 1(a) shows the average of 10 images taken under identical experimental conditions. Because of the symmetry of $V_r(x, y)$, and a precise calibration of the absorption imaging [42], we can azimuthally average these images to obtain $n(V_r)$ as shown in Fig. 1(b).

Both a and $V_r(x, y)$ are precisely known for a given experimental sequence providing accurate knowledge of E_b and, via the LDA, the change in chemical potential

$d\mu (\equiv -dV_r)$ across the cloud. Other parameters, however, including the absolute temperature and chemical potential, are unknown. Furthermore, absorption imaging is susceptible to systematics that make precise calibration of the atom density challenging [45–48]. To proceed we first obtain an estimate of the absolute temperature and chemical potential by fitting the low density wings of the cloud with the virial expansion in 2D to third order [49]. As only a small fraction of the cloud can be used, this can lead to relatively large uncertainties in the fits [42]. Fortunately, the relationships connecting f_p, f_n, and f_κ allow this to be improved. In analogy with Refs. [35,36], we use the $n(V_r)$ data to construct a model independent equation of state for the dimensionless compressibility $\tilde{\kappa} = \kappa/\kappa_0$ versus pressure $\tilde{p} = P/P_0$ [35] where $\kappa_0 = 1/(nE_F)$ and $P_0 = nE_F/2$ are the local compressibility and pressure of an ideal Fermi gas at $T = 0$, respectively, $E_F = (\hbar^2\pi/m)n = k_B T_F$ is the local Fermi energy, and T_F is the Fermi temperature. In Fig. 1(c) we plot $\tilde{\kappa}$ against $\tilde{p}$ for $\beta E_b = 0.26(2)$. At high temperatures the compressibility lies close to that for the ideal gas yet it deviates above this at lower temperatures (lower $\tilde{p}$). The virial expansion provides a reliable prediction of $\tilde{\kappa}$ for $\tilde{p} \gtrsim 6$. Equations (1)–(3), along with $d\mu = -dV_r$, then allow one to find the relative temperature $\tilde{T} = T/T_F$ and $\beta\mu$ at any position in the cloud using the integrals

$$\tilde{T} = \tilde{T}_i \exp\left[\frac{1}{2}\int_{\tilde{p}_i}^{\tilde{p}} \frac{d\tilde{p}'}{\tilde{p}' - \frac{1}{\tilde{\kappa}}}\right], \tag{4}$$

$$\beta\mu = (\beta\mu)_i - \int_{\tilde{T}_i}^{\tilde{T}} \frac{1}{\tilde{T}'^2}\left(\frac{1}{\tilde{\kappa}}\right)d\tilde{T}', \tag{5}$$

where the initial points can be chosen to lie in the range where the virial expansion is accurate. Implementation of Eq. (4) turns out to be relatively insensitive to the precise starting conditions and provides highly robust thermometry directly from the $\tilde{\kappa}$ vs $\tilde{p}$ equation of state. As a validation of the imaging calibration, the absolute temperature found from Eq. (4) should be consistent across the entire cloud and should match the value of βE_b that gave the best fit in the cloud wings using the virial expansion [42].

The integral for the chemical potential, Eq. (5), should also yield values of $\beta\mu$ that are consistent with the temperature found using Eq. (4). Additionally, μ should vary according to the LDA as a function of position across the cloud. Meeting all of these conditions requires accurate calibration of the absorption imaging as full consistency is only obtained with the correct parameters [42]. Agreement with the virial expansion at high temperatures provides a complementary validation of the thermodynamic parameters that assure the data are free from systematics within the error bounds of the virial fit.

With T/T_F and $\beta\mu$ known across the cloud, and the above criteria satisfied, we can construct the homogeneous
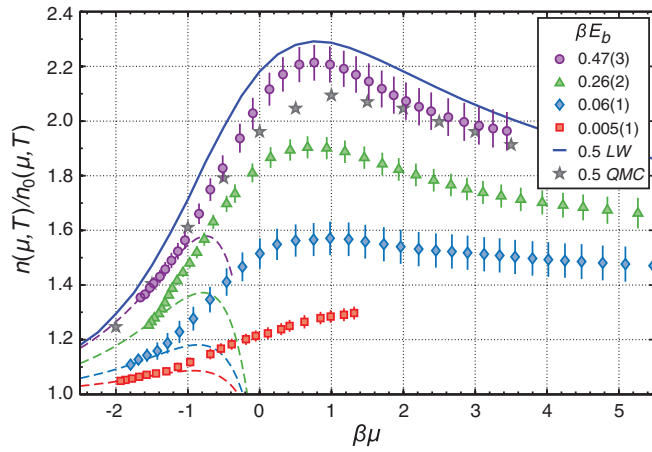
FIG. 2.   Normalized density equation of state for a 2D attractive Fermi gas for $\beta E_b = 0.47(3)$ (purple circles), $\beta E_b = 0.26(2)$ (green triangles), $\beta E_b = 0.06(1)$ (blue diamonds), and $\beta E_b = 0.005(1)$ (red squares). Dashed lines show the calculated equation of state using the third order virial expansion [49]. Solid blue line and grey stars are the calculated equation of state for $\beta E_b = 0.5$ based on Luttinger-Ward (LW) [26] and quantum Monte Carlo (QMC) calculations [27], respectively.
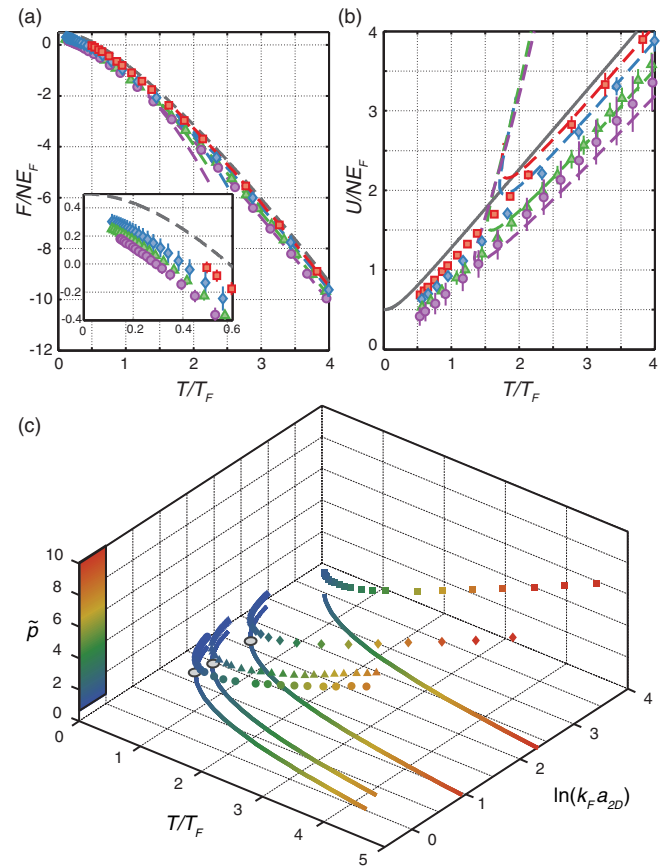

FIG. 3.   (a) Normalized free energy F and (b) internal energy U as a function of T/T_F for $\beta E_b = 0.47(3)$ (purple circles), $\beta E_b = 0.26(2)$ (green triangles), $\beta E_b = 0.06(1)$ (blue daimonds), and $\beta E_b = 0.005(1)$ (red squares). Inset in (a) shows a zoomed in view of F at low temperature. Dashed lines show the calculated energies using the virial expansion for the same values of βE_b and grey lines show the ideal gas result. (c) Normalized pressure $\tilde{p}$ as a function of the interaction parameter $\ln(k_F a_{2D})$ and temperature T/T_F. Solid lines show how the interaction parameter varies as a function of the relative temperature within single clouds and grey circles on the contours indicate the approximate location of the peak in $n(\mu,T)/n_0(\mu,T)$.

density equation of state. In Fig. 2 we plot $n(\mu,T)$ for four values of βE_b, normalized to the density of an ideal Fermi gas at the same chemical potential and temperature $n_0(\mu,T) = (2/\lambda^2)\ln(1+e^{\beta\mu})$. Reducing dimensionality leads to a dramatic difference in this equation of state compared to the 3D attractive Fermi gas [35,50]. The normalized density n/n_0 displays a nonmonotonic behavior as a function of $\beta\mu$. This is most evident for the gas with strongest interactions $\beta E_b = 0.47$ where n/n_0 peaks just below $\beta\mu = 1$. Also shown are the calculated equations of state using the virial expansion (dashed lines) [49], which is valid for $\beta\mu \lesssim -1.5$, along with recent Luttinger-Ward (LW, solid line) [26] and quantum Monte Carlo (QMC, grey stars) [27] calculations for a cloud with $\beta E_b = 0.5$. Our data for $\beta E_b = 0.47$ shows good qualitative agreement with these calculations lying in between the LW and QMC curves.

The peak in n/n_0 originates from the presence of a two-body bound state which exists for arbitrarily weak attraction in 2D. Interactions will generally be most significant when the kinetic energy of colliding atoms, E_k, is approximately equal to E_b. In 2D, when $T \ll T_F$, this occurs when the interaction parameter $\ln(k_F a_{2D}) \to 0$ [8], where $k_F = \sqrt{2\pi n}$ is the Fermi wave vector. At $T = 0$, the existence of a bound state leads to the possibility of tuning from the fermionic (BCS) regime where $E_b \ll E_F$, to the bosonic regime with $E_b \gg E_F$, simply by varying the density. At finite temperatures, the thermal energy $k_B T$ sets a lower bound on the collision energy and the Bose limit is only possible when $\beta E_b > 1$. For the data in Fig. 2, βE_b is always less than unity and E_k always exceeds E_b. In the low density (classical) region of the clouds, where $\beta\mu < 0$, E_k

will be set by $k_B T$, and interactions become stronger as the density begins increasing and the relative temperature $\tilde{T}$ decreases. However, once $\beta\mu \gtrsim 1$, E_F becomes the dominant energy (quantum regime) and E_k increases above $k_B T$, and hence further above E_b. This leads to effectively weaker interactions at high density and n/n_0 begins decreasing for $\beta\mu \gtrsim 1$.

Not all thermodynamic properties of an interacting 2D Fermi gas can be obtained from measurements on a single cloud. While the free energy, $F = U - TS$, where U is the internal energy and S is the entropy, is readily found via the grand potential $\Omega = -PA = F - \mu N$, where A is the area and N is the particle number, U and S cannot be found individually without further information. The normalized free energy is given by $F/(NE_F) \equiv \tilde{F} = \mu/E_F - \tilde{p}/2$, and

is plotted in Fig. 3(a). However, unique determination of U and S requires differentiation across clouds with different a_{2D}. Specifically, by considering $\tilde{F}$ as a function of temperature and a_{2D} we can evaluate the contact density $\mathcal{C}$ using $d\tilde{F}/d(\ln a_{2D}) = 2\mathcal{C}/k_F^4$ at fixed T/T_F. With this the internal energy, and hence the entropy, can be found via the Tan pressure relation [51–53], $\tilde{p} = 2U/(NE_F) + 2\mathcal{C}/k_F^4$ [42]. As we only have measurements at four values of a_{2D} the measured contact contains significant uncertainty compared to other variables. However, as $\mathcal{C}$ remains relatively small in our experiments, the internal energy shows the expected behavior, Fig. 3(b).

Finally, we can plot the dimensionless pressure $\tilde{p}$ versus interactions and temperature in Fig. 3(c). Constructing a full 3D surface plot of $\tilde{p}$ as a function of $\ln(k_F a_{2D})$ and T/T_F would represent a complete characterization of the thermodynamics of the 2D Fermi gas. The contours in the $\tilde{p} = 0$ plane show how the relative temperature and interaction strength evolve in a single cloud. Grey circles on the contours indicate the approximate peak location in the density equation of state.

In summary we have measured the thermodynamic properties of a 2D Fermi gas with attractive interactions in the normal phase. The existence of a bound state leads to qualitatively different behavior to 3D gases as apparent in the density equation of state. For the gas with strongest interactions ($\beta E_b = 0.47$) the superfluid transition temperature is expected to lie at approximately $0.05 T/T_F$ [26] which is around a factor of 2 colder than we currently achieve. Future studies investigating thermodynamic signatures of the superfluid transition may provide insight into the nature of the transition in a quasi-2D Fermi gas. At stronger interactions one could investigate the effects of transverse excitations on the thermodynamic properties.

Note added.—A related work has recently been posted which examines the thermodynamic equation of state across the 2D BEC-BCS crossover [54].

———————————

*To whom all correspondence should be addressed.
cvale@swin.edu.au

[1] N. D. Mermin and H. Wagner, Phys. Rev. Lett. **17**, 1133 (1966).
[2] P. C. Hohenberg, Phys. Rev. **158**, 383 (1967).
[3] E. Dagotto, Rev. Mod. Phys. **66**, 763 (1994).
[4] A. K. Geim and K. S. Novoselov, Nat. Mater. **6**, 183 (2007).
[5] M. Z. Hasan and C. L. Kane, Rev. Mod. Phys. **82**, 3045 (2010).
[6] I. Bloch, J. Dalibard, and W. Zwerger, Rev. Mod. Phys. **80**, 885 (2008).
[7] *BCS-BEC Crossover and the Unitary Fermi Gas*, edited by W. Zwerger, Lecture Notes in Physics (Springer, New York, 2012).
[8] J. Levinsen and M. M. Parish, Annu. Rev. Cold Atoms and Molecules **3**, 1 (2015).
[9] G. Modugno, F. Ferlaino, R. Heidemann, G. Roati, and M. Inguscio, Phys. Rev. A **68**, 011601 (2003).
[10] K. Martiyanov, V. Makhalov, and A. Turlapov, Phys. Rev. Lett. **105**, 030404 (2010).
[11] P. Dyke, E. D. Kuhnle, S. Whitlock, H. Hu, M. Mark, S. Hoinka, M. Lingham, P. Hannaford, and C. J. Vale, Phys. Rev. Lett. **106**, 105304 (2011).
[12] B. Fröhlich, M. Feld, E. Vogt, M. Koschorreck, W. Zwerger, and M. Köhl, Phys. Rev. Lett. **106**, 105301 (2011).
[13] A. T. Sommer, L. W. Cheuk, M. J. H. Ku, W. S. Bakr, and M. W. Zwierlein, Phys. Rev. Lett. **108**, 045302 (2012).
[14] M. Feld, B. Fröhlich, E. Vogt, M. Koschorreck, and M. Köhl, Nature (London) **480**, 75 (2011).
[15] M. Koschorreck, D. Pertot, E. Vogt, B. Fröhlich, M. Feld, and M. Köhl, Nature (London) **485**, 619 (2012).
[16] Y. Zhang, W. Ong, I. Arakelyan, and J. E. Thomas, Phys. Rev. Lett. **108**, 235302 (2012).
[17] M. G. Ries, A. N. Wenz, G. Zürn, L. Bayha, I. Boettcher, D. Kedar, P. A. Murthy, M. Neidig, T. Lompe, and S. Jochim, Phys. Rev. Lett. **114**, 230401 (2015).
[18] P. A. Murthy, I. Boettcher, L. Bayha, M. Holzmann, D. Kedar, M. Neidig, M. G. Ries, A. N. Wenz, G. Zürn, and S. Jochim, Phys. Rev. Lett. **115**, 010401 (2015).
[19] V. Makhalov, K. Martiyanov, and A. Turlapov, Phys. Rev. Lett. **112**, 045301 (2014).
[20] D. S. Petrov, M. A. Baranov, and G. V. Shlyapnikov, Phys. Rev. A **67**, 031601(R) (2003).
[21] J.-P. Martikainen and P. Törmä, Phys. Rev. Lett. **95**, 170407 (2005).
[22] S. S. Botelho and C. A. R. Sá de Melo, Phys. Rev. Lett. **96**, 040404 (2006).
[23] W. Zhang, G. D. Lin, and L.-M. Duan, Phys. Rev. A **78**, 043617 (2008).
[24] A. M. Fischer and M. M. Parish, Phys. Rev. B **90**, 214503 (2014).
[25] G. Bertaina and S. Giorgini, Phys. Rev. Lett. **106**, 110403 (2011).
[26] M. Bauer, M. M. Parish, and T. Enss, Phys. Rev. Lett. **112**, 135302 (2014).
[27] E. R. Anderson and J. E. Drut, Phys. Rev. Lett. **115**, 115301 (2015).
[28] D. S. Petrov and G. V. Shlyapnikov, Phys. Rev. A **64**, 012706 (2001).
[29] Z. Idziaszek and T. Calarco, Phys. Rev. A **71**, 050701(R) (2005).
[30] J. P. Kestner and L.-M. Duan, Phys. Rev. A **74**, 053606 (2006).
[31] E. Haller, M. J. Mark, R. Hart, J. G. Danzl, L. Reichsöllner, V. Melezhik, P. Schmelcher, and H.-C. Nägerl, Phys. Rev. Lett. **104**, 153203 (2010).
[32] S. Sala, P.-I. Schneider, and A. Saenz, Phys. Rev. Lett. **109**, 073201 (2012).

[33] P. Dyke, K. Fenech, T. Peppler, M. G. Lingham, S. Hoinka, W. Zhang, S.-G. Peng, B. Mulkerin, H. Hu, X.-J. Liu, and C. J. Vale, Phys. Rev. A **93**, 011603(R) (2016).

[34] A. M. Fischer and M. M. Parish, Phys. Rev. A **88**, 023612 (2013).

[35] M. J. H. Ku, A. T. Sommer, L. W. Cheuk, and M. W. Zwierlein, Science **335**, 563 (2012).

[36] R. Desbuquois, T. Yefsah, L. Chomaz, C. Weitenberg, L. Corman, S. Nascimbène, and J. Dalibard, Phys. Rev. Lett. **113**, 020404 (2014).

[37] T.-L. Ho, Phys. Rev. Lett. **92**, 090402 (2004).

[38] K. Van Houcke, F. Werner, E. Kozik, N. Prokof'ev, B. Svistunov, M. J. H. Ku, A. T. Sommer, L. W. Cheuk, A. Schirotzek, and M. W. Zwierlein, Nat. Phys. **8**, 366 (2012).

[39] F. Dalfovo, S. Giorgini, L. P. Pitaevskii, and S. Stringari, Rev. Mod. Phys. **71**, 463 (1999).

[40] N. L. Smith, W. H. Heathcote, G. Hechenblaikner, E. Nugent, and C. J. Foot, J. Phys. B **38**, 223 (2005).

[41] S. P. Rath, T. Yefsah, K. J. Günter, M. Cheneau, R. Desbuquois, M. Holzmann, W. Krauth, and J. Dalibard, Phys. Rev. A **82**, 013609 (2010).

[42] See Supplemental Material at http://link.aps.org/supplemental/10.1103/PhysRevLett.116.045302 for further information on cloud preparation, calibration of absorption imaging, and full details of data analysis, which includes Refs. [43,44].

[43] X. Leyronas, Phys. Rev. A **84**, 053633 (2011).

[44] V. Ngampruetikorn, J. Levinsen, and M. M. Parish, Phys. Rev. Lett. **111**, 265301 (2013).

[45] G. Reinaudi, T. Lahaye, Z. Wang, and D. Guéry-Odelin, Opt. Lett. **32**, 3143 (2007).

[46] T. Yefsah, R. Desbuquois, L. Chomaz, K. J. Günter, and J. Dalibard, Phys. Rev. Lett. **107**, 130401 (2011).

[47] L. Chomaz, L. Corman, T. Yefsah, R. Desbuquois, and J. Dalibard, New J. Phys. **14**, 055001 (2012).

[48] C.-L. Hung and C. Chin, in *Quantum Gas Experiments: Exploring Many-Body States*, edited by P. Törmä and K. Sengstock (World Scientific, Singapore, 2014).

[49] X.-J. Liu, H. Hu, and P. D. Drummond, Phys. Rev. B **82**, 054524 (2010).

[50] S. Nascimbène, N. Navon, K. J. Jiang, F. Chevy, and C. Salomon, Nature (London) **463**, 1057 (2010).

[51] J. Hofmann, Phys. Rev. Lett. **108**, 185303 (2012).

[52] F. Werner and Y. Castin, Phys. Rev. A **86**, 013626 (2012).

[53] M. Valiente, N. T. Zinner, and K. Mølmer, Phys. Rev. A **86**, 043616 (2012).

[54] I. Boettcher, L. Bayha, D. Kedar, P. A. Murthy, M. Neidig, M. G. Ries, A. N. Wenz, G. Zürn, S. Jochim, and T. Enss, following Letter, Phys. Rev. Lett. **116**, 045303 (2016).